Recent results in the HAL QCD method

Sinya Aoki

Center for Gravitational Physics and Quantum Information,
Yukawa Institute for Theoretical Physics, Kyoto University

for
HAL QCD collaboration

"Challenge and opportunities in Lattice QCD simulations and related fields"
15-17 February, 2023, RIKEN R-CCS, Kobe, Japan

I dedicate this talk to a memory of Prof. Yoichi Iwasaki, who has just passed away on February 2nd, 2023.

Yoichi Iwasaki
1941/9/12 ~ 2023/2/2

Yoichi had been my collage at University of Tsukuba, and a founder of lattice QCD in Japan. While he is famous as QCD-PAX and CP-PACS project leader, I think he is also a great theoretical physicist. Peter Hasenfratz said to me once “When I though I found a great idea, later I have always realized that Prof. Iwasaki already had same idea, for example, RG improvement, NL sigma model, etc.”

I will miss Yoichi with my deepest sympathy.

I. Introduction

Hadron interactions in lattice QCD

Finite volume (FV) method

spectra of two hadrons
in finite box

scattering phase shift

Luescher's finite volume formula

HAL QCD method

NBS wave functions

Potential
(Interaction kernel)

scattering
phase shift

Schrodinger equation

It is always better to have two "different" methods for crosschecks.

NN controversy

FV spectra: both deuteron and dineutron are bound at heavier pion masses.

Potential : Two nucleons are unbound at heavier pion masses.

Fortunately, lattice QCD community's efforts are resolving controversy.

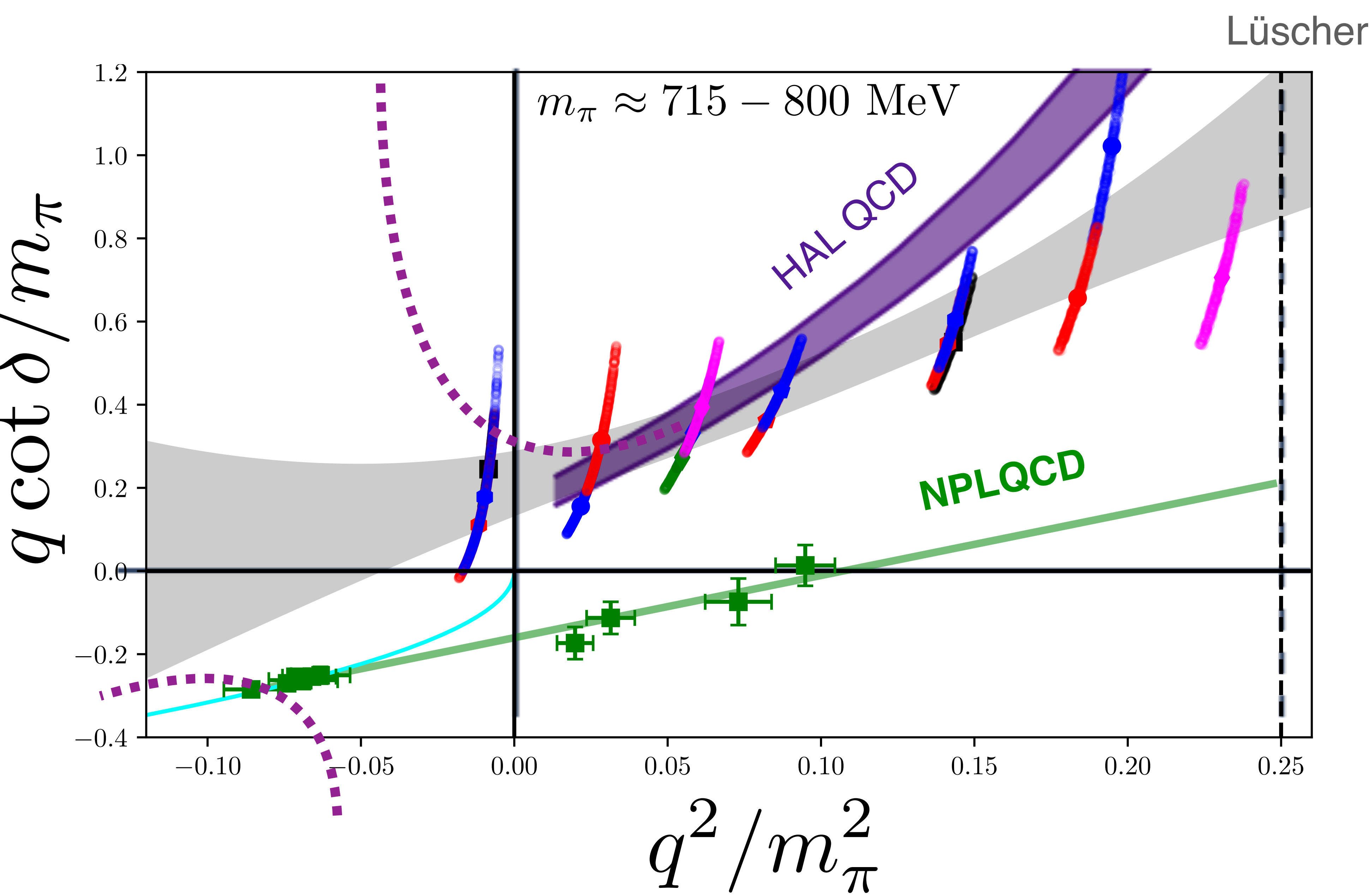

A. Nicolson, Lat2022

It is very unlikely to miss a bound state.

Community's consensus

Latest FV spectra are consistent with potential results at low energy.

Two nucleons are unbound at heavy pion masses.

Today’s topics

I. Introduction

II. HAL QCD method

1. Formulation

2. Comparison: FV and HAL QCD methods

III. Potentials and FV spectra

1. Recent results for heavy dibaryons

2. Finite volume spectra with projections

IV. Conclusions

II. HAL QCD method

N. Ishii, S. Aoki, T. Hatsuda, PRL99(2007) 022001.
S. Aoki, T. Hatsuda, N. Ishii, PTP123(2010)89-128.
HAL QCD Collaboration (S.Aoki et al.), PTEP2012(2012) 01A105.

1. Formulation

Nambu-Bethe-Salpeter (NBS) wave function

vacuum

$$\psi_W^{H_1+H_2}(\mathbf{r},t) \equiv \psi_W^{H_1+H_2}(\mathbf{r})\, e^{-Wt} \equiv \frac{1}{\sqrt{Z_{H_1}}}\frac{1}{\sqrt{Z_{H_2}}}\sum_{\mathbf{x}} \langle\Omega|\, H_1(\mathbf{x}+\mathbf{r},t) H_2(\mathbf{x},t)\, |(H_1+H_2);W\rangle\,,$$

hadron ops. QCD eigenstate

Center of mass energy $\quad W = \sqrt{\mathbf{p}_W^2 + m_{H_1}^2} + \sqrt{\mathbf{p}_W^2 + m_{H_2}^2}$

Large r behavior

$$\psi_W^{H_1+H_2}(\mathbf{r}) \propto \frac{\sin(p_W r + \delta_l(p_W) - l\pi/2)}{p_W r} P_l(\cos(\theta)) \qquad \mathbf{p}_W\cdot\mathbf{r} = p_W r\cos\theta$$

$$\delta_\ell(p_W)\,:\ \text{phase shift of } \ell\text{-th partial wave}$$

NBS wave function encodes information of scattering phase shifts in its asymptotic behavior, as in the case of quantum mechanics.

FV method also uses property.

Non-local potential

$$\left(\frac{\nabla^2}{2\mu}+\frac{p_W^2}{2\mu}\right)\psi_W(\mathbf{r})=\int \mathrm{d}^3\mathbf{r}'\,U(\mathbf{r},\mathbf{r}')\psi_W(\mathbf{r}'),$$

μ: reduced mass

non-local potential

derivative expansion $U(\mathbf{r},\mathbf{r}')=V(\mathbf{r},\nabla)\delta(\mathbf{r}-\mathbf{r}')=\sum_{k=0}^{\infty}V^{(k)}(\mathbf{r})\nabla^k\delta(\mathbf{r}-\mathbf{r}')$

$$V^{(0)}(\mathbf{r};W)=\frac{1}{\psi_W(\mathbf{r})}\left(\frac{\nabla^2}{2\mu}+\frac{p_W^2}{2\mu}\right)\psi_W(\mathbf{r})$$

leading order (LO) potential

This introduces some systematics.

$\longrightarrow$ $\delta_\ell(q=p_W)$ Exact "anchor"

$\longrightarrow$ $\delta_\ell(q\neq p_W)$ Approximate

$k\cot(\delta_0(k))$

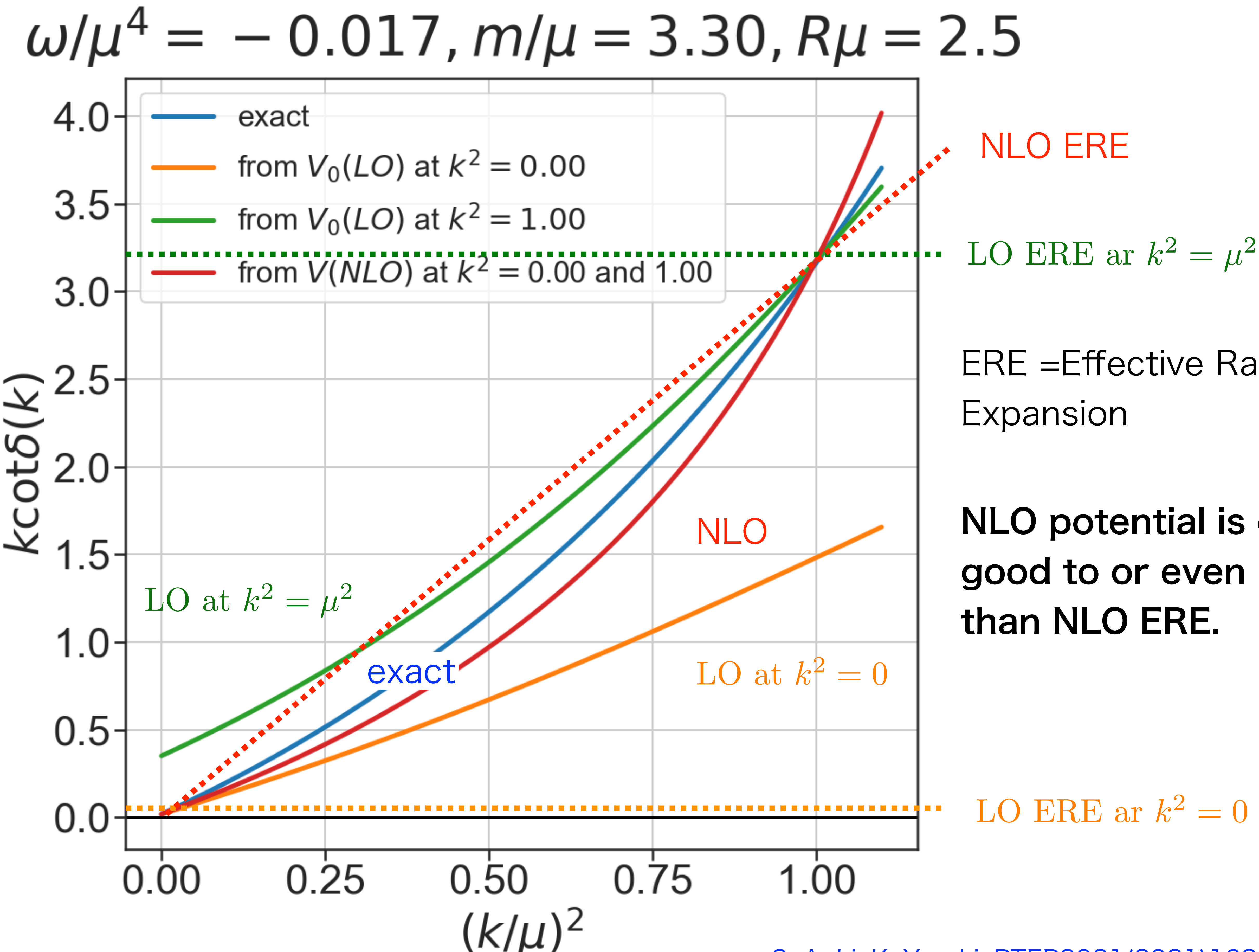

ERE =Effective Range Expansion

NLO potential is equally good to or even better than NLO ERE.

S. Aoki, K. Yazaki, PTEP2021(2021)168, 033B04.

4-pt correlation function $\longrightarrow$ NBS wave function for a ground state

$$F_{\mathcal{J}}^{H_1+H_2}(\mathbf{r},t) \equiv \sum_{\mathbf{x}} \langle\Omega|\, H_1(\mathbf{x}+\mathbf{r},t)H_2(\mathbf{x},t)\mathcal{J}^{\dagger}_{H_1+H_2}(t=0)\,|\Omega\rangle \quad \xrightarrow{t\to\infty} \quad \mathcal{A}_{\mathcal{J},0}\psi_{W_0}^{H_1+H_2}(\mathbf{r})\, e^{-W_0 t}$$

source op.

In practice, however, it is difficult to take large t with small errors.

FV method also suffers from this problem.

Time-dependent method

Ishii et al. (HAL QCD), PLB712(2012)437

normalized 4-pt function (R-correlator)

$$R_{\mathcal{J}}^{H_1+H_2}(\mathbf{r},t) \equiv \frac{F_{\mathcal{J}}^{H_1+H_2}(\mathbf{r},t)}{e^{-m_{H_1}t}e^{-m_{H_2}t}} \simeq \sum_n \mathcal{A}_{\mathcal{J},n}\psi_{W_n}^{H_1+H_2}(\mathbf{r})\, e^{-\Delta W_n t}$$

NBS wave function

large t to surpress inelastic contributions

$\Delta W_n \equiv W_n - m_{H_1} - m_{H_2}$ satisfies $\quad \frac{p_n^2}{2\mu} = \Delta W_n + \frac{1+3\delta^2}{8\mu}(\Delta W_n)^2 + \mathcal{O}((\Delta W_n)^3), \qquad \delta \equiv \frac{|m_{H_1} - m_{H_2}|}{m_{H_1} + m_{H_2}}$

$$\int d^3\mathbf{r}'\, U(\mathbf{r},\mathbf{r}') R_{\mathcal{J}}^{H_1+H_2}(\mathbf{r}',t) \simeq \sum_n \left(\frac{\nabla^2}{2\mu} + \frac{p_n^2}{2\mu}\right) A_n^{\mathcal{J}}\psi_{W_n}^{H_1+H_2}(\mathbf{r})\, e^{-\Delta W_n t}$$

$$\simeq \sum_n \left(\frac{\nabla^2}{2\mu} + \Delta W_n + \frac{1+3\delta^2}{8\mu}(\Delta W_n)^2\right) A_n^{\mathcal{J}}\psi_{W_n}^{H_1+H_2}(\mathbf{r})\, e^{-\Delta W_n t}$$

$$= \left(\frac{\nabla^2}{2\mu} - \frac{\partial}{\partial t} + \frac{1+3\delta^2}{8\mu}\frac{\partial^2}{\partial t^2}\right) R_{\mathcal{J}}^{H_1+H_2}(\mathbf{r},t),$$

We have an exact formula for the time-dependent method if we use $\frac{\partial^3}{\partial t^3}$.

$$V^{(0)}(\mathbf{r}) = \frac{1}{R_{\mathcal{J}}^{H_1+H_2}(\mathbf{r},t)}\left(\frac{\nabla^2}{2\mu} - \frac{\partial}{\partial t} + \frac{1+3\delta^2}{8\mu}\frac{\partial^2}{\partial t^2}\right) R_{\mathcal{J}}^{H_1+H_2}(\mathbf{r},t).$$

LO potential

We don't need a ground-state saturation, but

We don't have an anchor $\delta_\ell(q = p_W)$ anymore.

HAL QCD potential method extension

Extensions to coupled channels are straightforward without assumptions.

Extensions to more than 3 particles are possible only for non-relativistic kinematics.

Enough for 3 nucleon forces. T. Doi et al. (HAL QCD), PTP127(2012)723

Relativistic extensions are desirable.

Extensions to moving frames are possible and indeed work for simple systems.

Y. Akahosi and S. Aoki, arXiv:2301.06038

2. Comparison: FV and HAL QCD methods

Finite volume method	HAL QCD method
Exact $\delta_\ell(p_W)$ at each p_W.	Exact $\delta_\ell(p_W)$ and approximated $\delta_\ell(q)$ at once with some physical pictures.
More data, more exact $\delta_\ell(q)$.	Improvable by the derivative expansion.
Correct spectra are essential in practice.	Time-dependent method helps, while anchors are lost.
More results on mesons.	More results on baryons.
Center of Mass (CM) frame as well as moving ones.	Mainly CM. Moving frame available.
Models/assumptions are required for couple channel extensions.	Coupled channel extension is easy.
Many multi-particle formalisms.	Multi-particles only for NR particles.

We may combine both methods to improve accuracy and precision.
Let us demonstrate it.

III. Potentials and finite volume spectra

1. Recent results for heavy dibaryons

Dibaryons

Baryon (B=1)

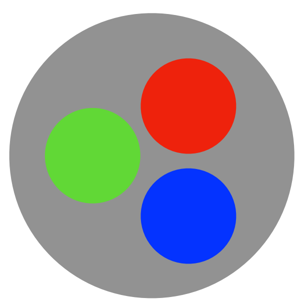

Proton, Neutron,
Lambda, Omega,…

Dibaryon (B=2)

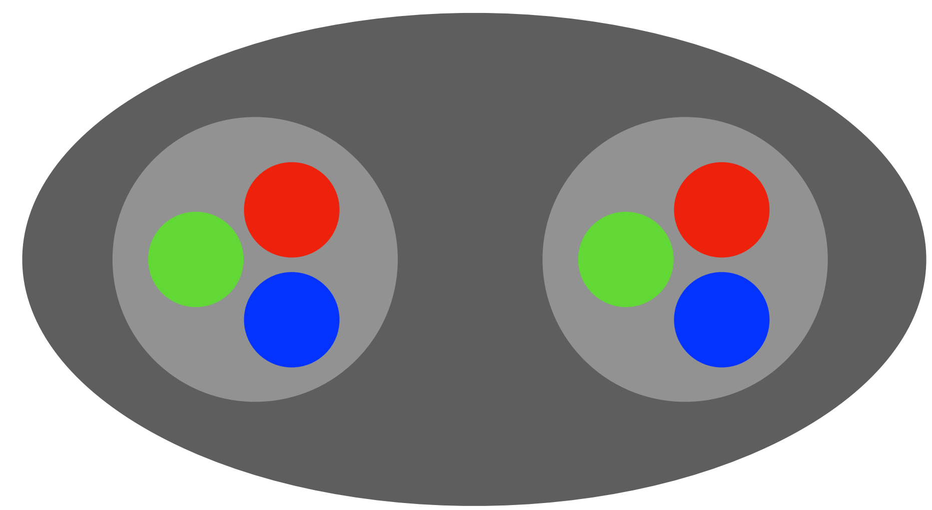

Deuteron
observed in 1930s
+ d*(2380) resonance

Dibaryon = two baryon bound state or resonance

HAL QCD results on dibaryons

H dibaryon

T. Inoue et al. (HAL QCD Coll.), PRL106(2011)162002 — flavor SU(3) limit

K. Sasaki et al. (HAL QCD Coll.), NPA106(2020)121737 — physical point, $\Lambda\Lambda - N\Xi$ coupled channel

$\Delta\Delta$ dibaryon

S. Gongyo et al. (HAL QCD Coll.), PLB811(2020)135935 — flavor SU(3) limit, $d^*(2380)$

$N\Omega$ dibaryon

F. Etminan et al. (HAL QCD Coll.), NPA928(2014)89 — $m_\pi \simeq$ 875 MeV

T. Iritani et al. (HAL QCD Coll.), PLB792(2019)284 — physical point

$\Omega\Omega$ dibaryon

M. Yamada et al. (HAL QCD Coll.), PTEP 7(2015)187 — $m_\pi \simeq$ 700 MeV

S. Gongyo et al. (HAL QCD Coll.), PRL 120(2018)212001 — physical point

$\Omega_{ccc}\Omega_{ccc}$ dibaryon

Y. Lyu et al. (HAL QCD Coll.), PRL 127 (2021) 072003 — physical point

Physical point configurations

2+1 flavor gauge configuration on 96^4 lattice

with Iwasaki gauge + NP $O(a)$ improved clover quark

$a \simeq 0.0846$ fm, $m_\pi \simeq 146$ MeV, $m_K \simeq 525$ MeV (near physical point)

$La \simeq 8.1$ fm

(quenched) charm quark mass for Ω_{ccc}

	$(m_{\eta_c} + 3m_{J/\Psi})/4$ [MeV]	$m_{\Omega_{ccc}}$ [MeV]
set 1	3096.6(0.3)	4837.3(0.7)
set 2	3051.4(0.3)	4770.2(0.7)
Interpolation	3068.5(0.3)	4795.6(0.7)
Exp.	3068.5(0.1)	-

Potentials

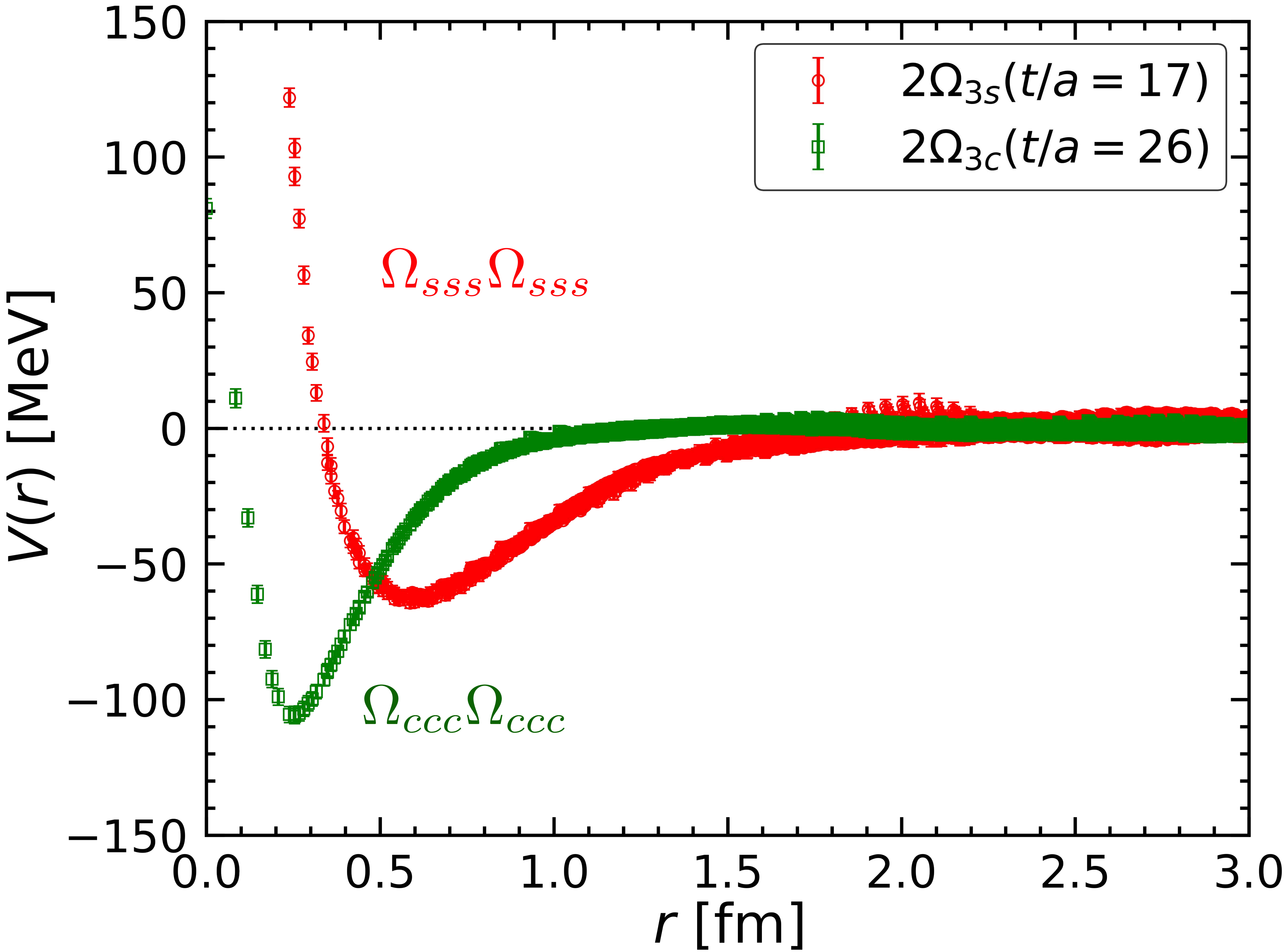

Attraction is wider and repulsive core is larger for Ω_{sss} than Ω_{ccc}.

Potentials (3-dim plot)

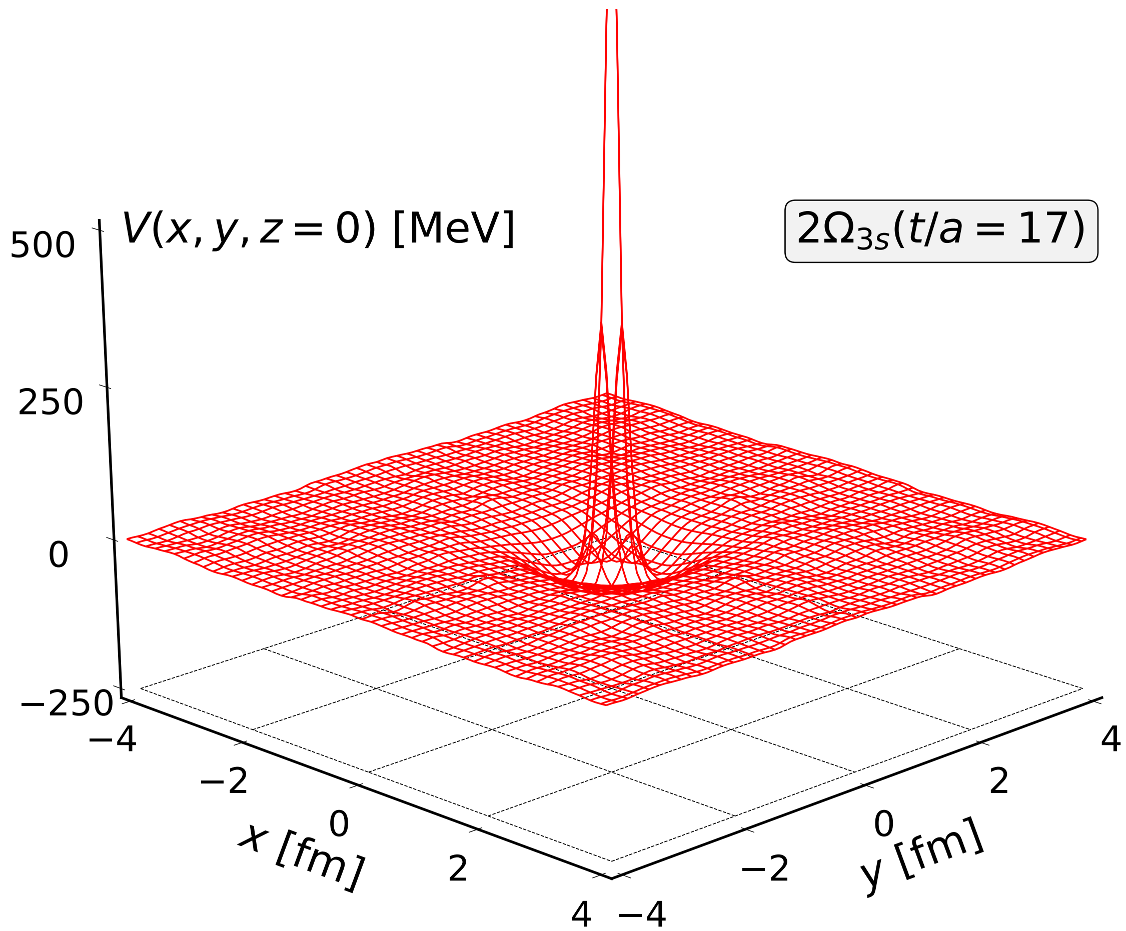

$\Omega_{sss}\Omega_{sss}$

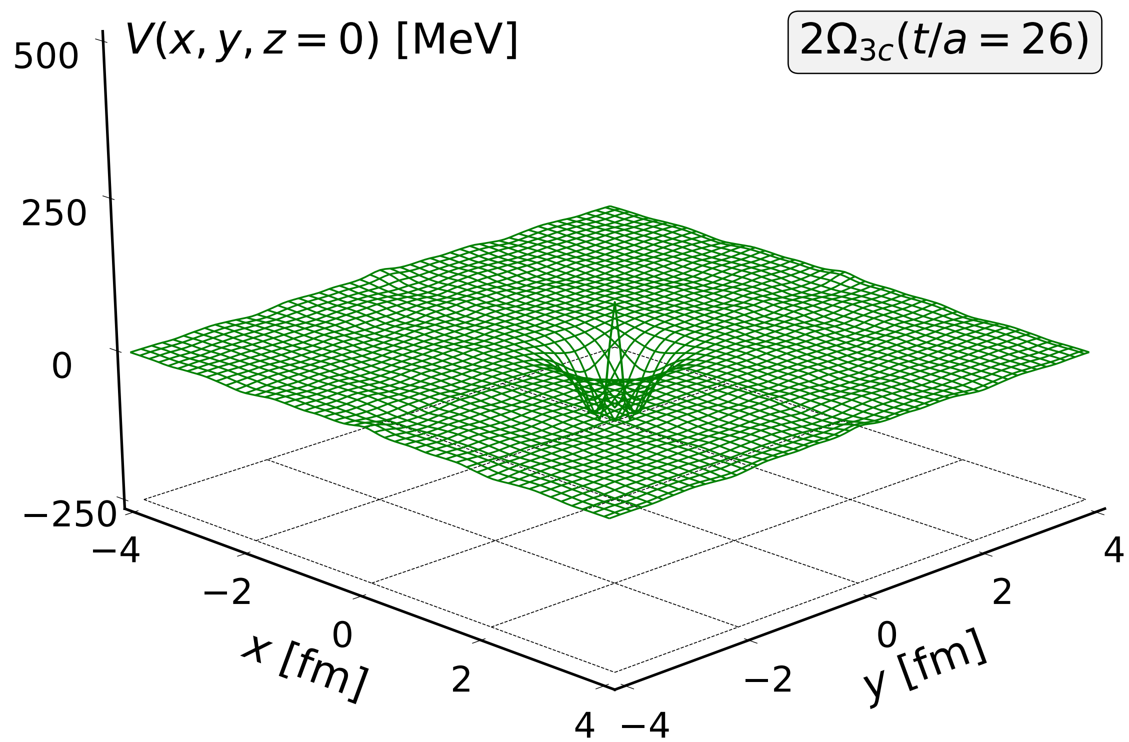

$\Omega_{ccc}\Omega_{ccc}$

Repulsive core surrounded by an attractive pocket.

Scattering phase shift

$\Omega_{sss}\Omega_{sss}$

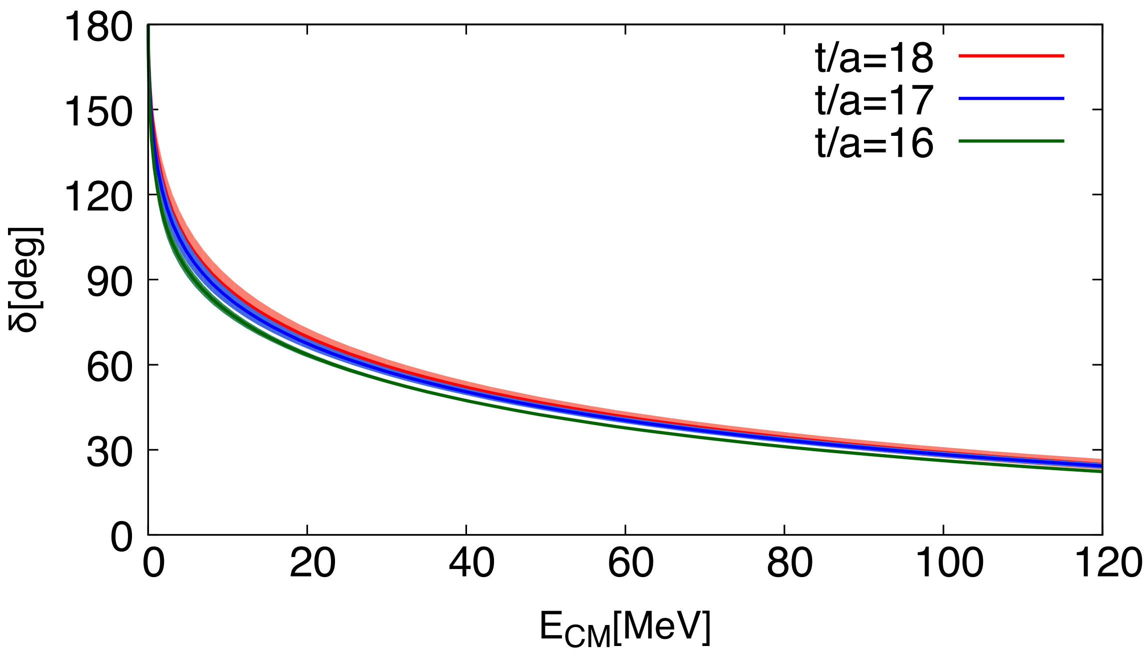

$\Omega_{ccc}\Omega_{ccc}$

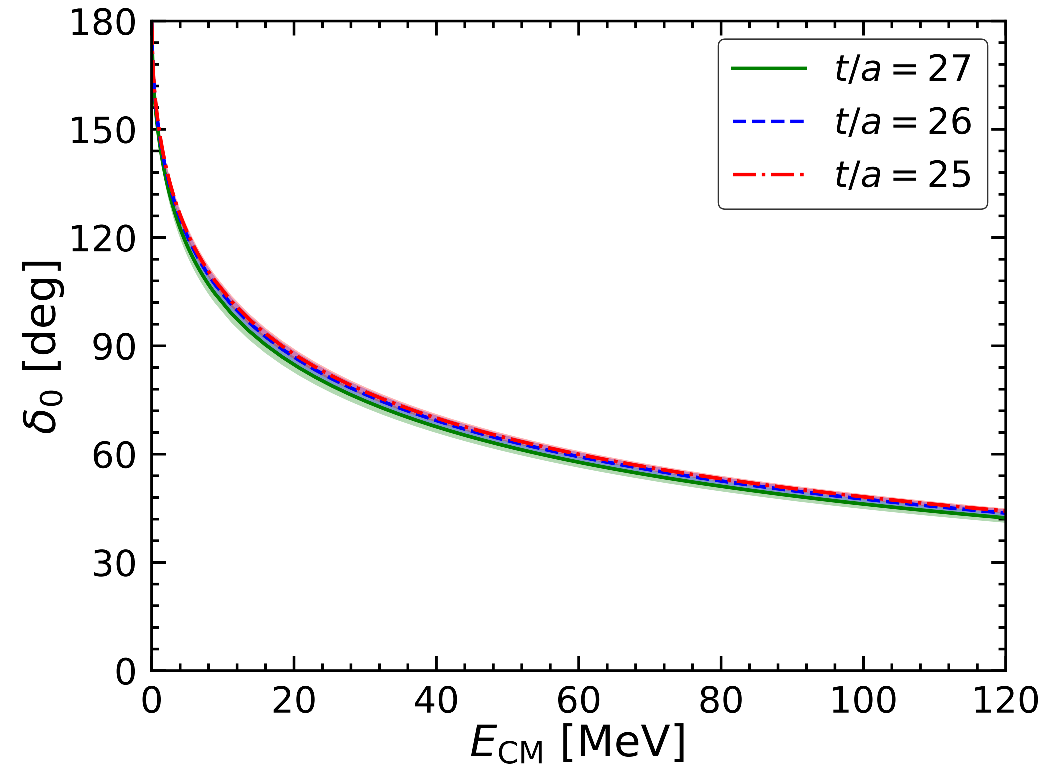

Effective Range Expansion (ERE)

$$k \cot \delta_0(k) = -\frac{1}{a_0} + \frac{1}{2} r_{\text{eff}} k^2 + O(k^4)$$

scattering length

$$a_0^{(\Omega\Omega)} = 4.6(6)\left(^{+1.2}_{-0.5}\right) \quad \text{fm},$$

$$a_0 = 1.57(0.08)\left(^{+0.12}_{-0.04}\right) \text{ fm},$$

effective range

$$r_{\text{eff}}^{(\Omega\Omega)} = 1.27(3)\left(^{+0.06}_{-0.03}\right) \quad \text{fm}.$$

$$r_{\text{eff}} = 0.57(0.02)\left(^{+0.01}_{-0.00}\right) \text{ fm}.$$

one bound state in each channel

Binding energy

$\Omega_{sss}\Omega_{sss}$ charge -1

binding energy $B = 1.6(0.6)(^{+0.7}_{-0.6})$ MeV

Coulomb repulsion
(point-like)

$$B_{\Omega\Omega}^{(\mathrm{QCD+Coulomb})} = 0.7(5)(5) \text{ MeV}$$

$\Omega_{ccc}\Omega_{ccc}$ charge +2

$B = 5.65(0.77)(^{+0.46}_{-0.03})$ MeV

Coulomb repulsion
(charge distribution)

unbound

unitary region

$$a_0^{\mathrm{C}} = -19(7)(^{+7}_{-6}) \text{ fm},$$
$$r_{\mathrm{eff}}^{\mathrm{C}} = 0.45(0.01)(^{+0.01}_{-0.00}) \text{ fm}.$$

$$r_{\mathrm{eff}}^{C}/a_0^{C} = -0.024(0.010)(^{+001}_{-0.00}) \text{ fm}$$

w/o Coulomb

$$a_0 = 1.57(0.08)(^{+0.12}_{-0.04}) \text{ fm},$$
$$r_{\mathrm{eff}} = 0.57(0.02)(^{+0.01}_{-0.00}) \text{ fm}.$$

Coulomb repulsion with charge distribution

charge distribution inside Ω_{ccc}

$$\rho(r) = \frac{12\sqrt{6}}{\pi r_d^3} \exp\left[-\frac{2\sqrt{6}r}{r_d}\right]$$

charge radius of Ω_{ccc} $r_d = 0.410(6)$ fm

K. U. Can, et al., Phys. Rev. D92 (2015) 114515.

Coulomb potential between two Ω_{ccc} 's

$$V^{\mathrm{Coulomb}}(r) = \alpha_e \iint d^3r_1 d^3r_2 \frac{\rho(r_1)\rho(|\vec{r}_2 - \vec{r}|)}{|\vec{r}_1 - \vec{r}_2|}$$

$1/a_0^C$ vs. $\alpha_e/\alpha_e^{\mathrm{phys.}}$

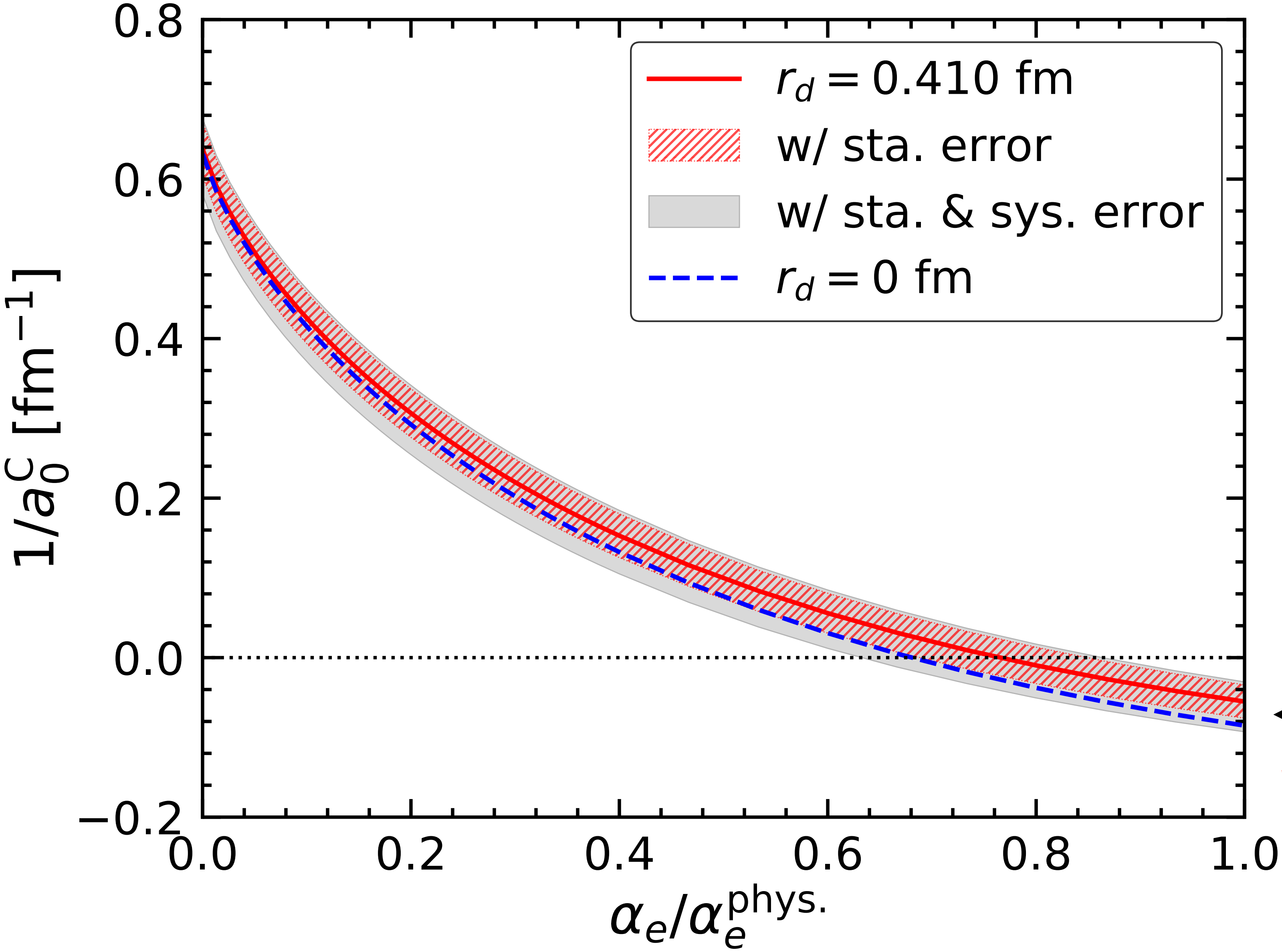

$$a_0^{\mathrm{C}} = -19(7)(^{+7}_{-6})\ \mathrm{fm},$$ unitary region

$$r_{\mathrm{eff}}^{\mathrm{C}} = 0.45(0.01)(^{+0.01}_{-0.00})\ \mathrm{fm}.$$

$r_{\mathrm{eff}}^C/a_0^C = -0.024(0.010)(^{+001}_{-0.00})$ fm

Comparison with other dibaryons

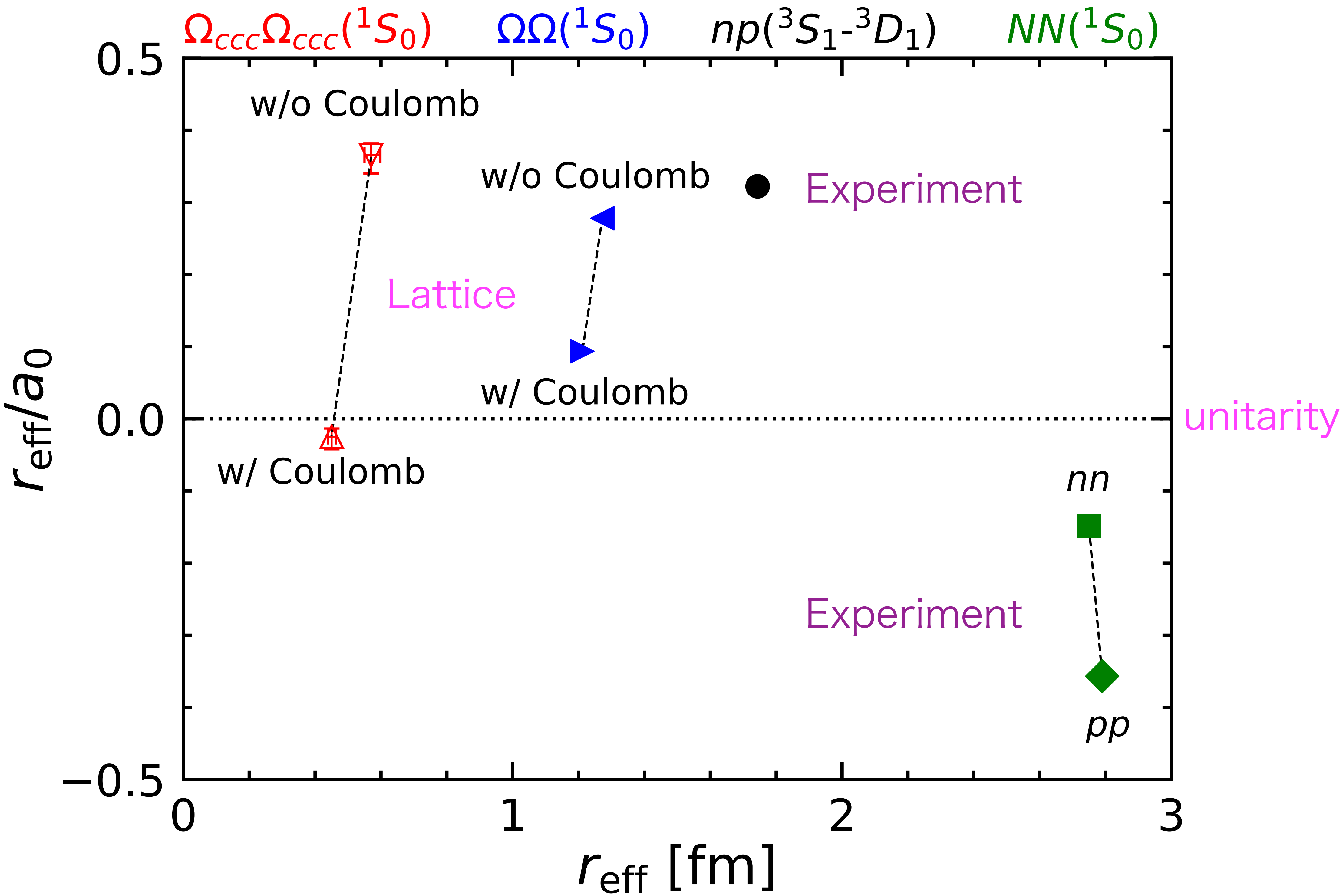

All “dibaryons” appear near unitarity. Why ?

$\Omega_{ccc}\Omega_{ccc}(^1S_0)$ dibaryon is closest to unitarity among these.

2. Finite volume spectra with projection

Y. Lyu et al. (HAL QCD collaboration), PRD105(2022) 074512.

HAL QCD potential in a box

$$H = H_0 + V(\mathbf{r}) \qquad V(\mathbf{r})\text{: raw data for } \Omega_{xxx}\Omega_{xxx} \text{ potential } (x = s, c)$$

finite dimensional Hermitian matrix $\longrightarrow$ Eigenvalues and eigenfunctions

$\Omega_{sss}\Omega_{sss}$ $\Omega_{ccc}\Omega_{ccc}$

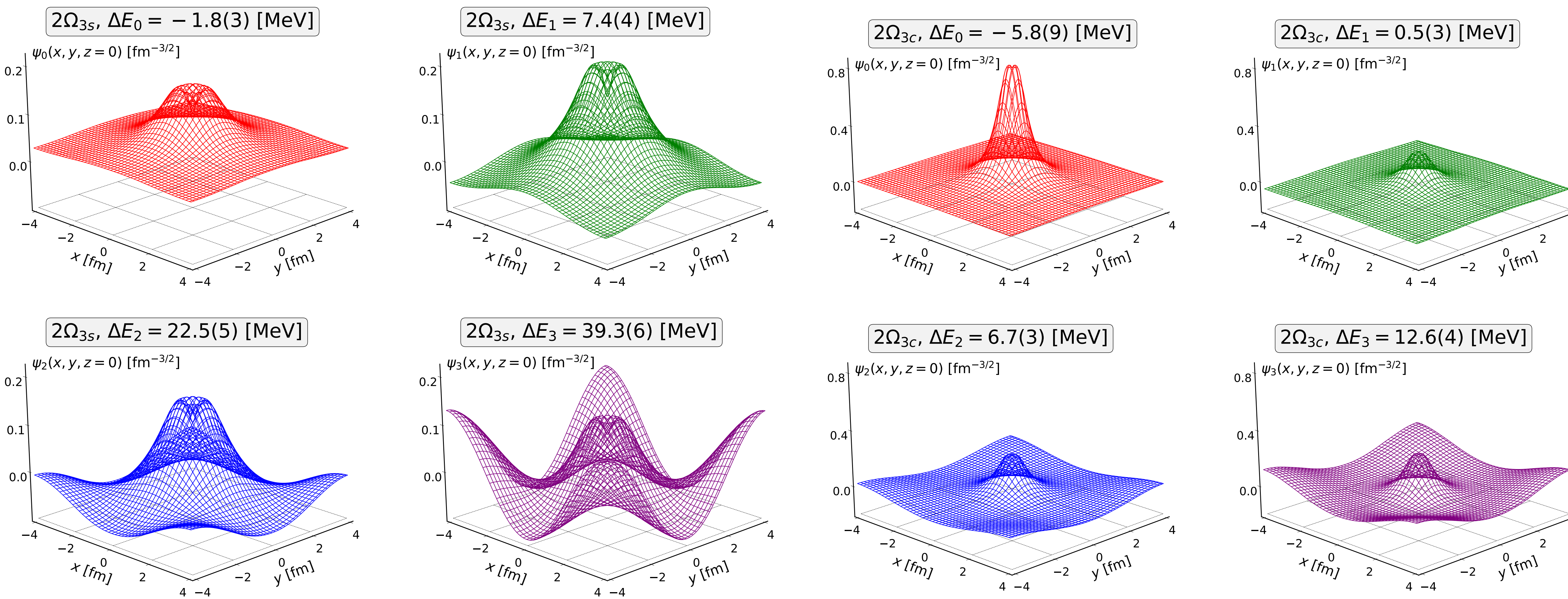

Lowest 4 eigenenergy and normalized eigenfunction $\psi_n(x, y, z = 0)$ in A_1.

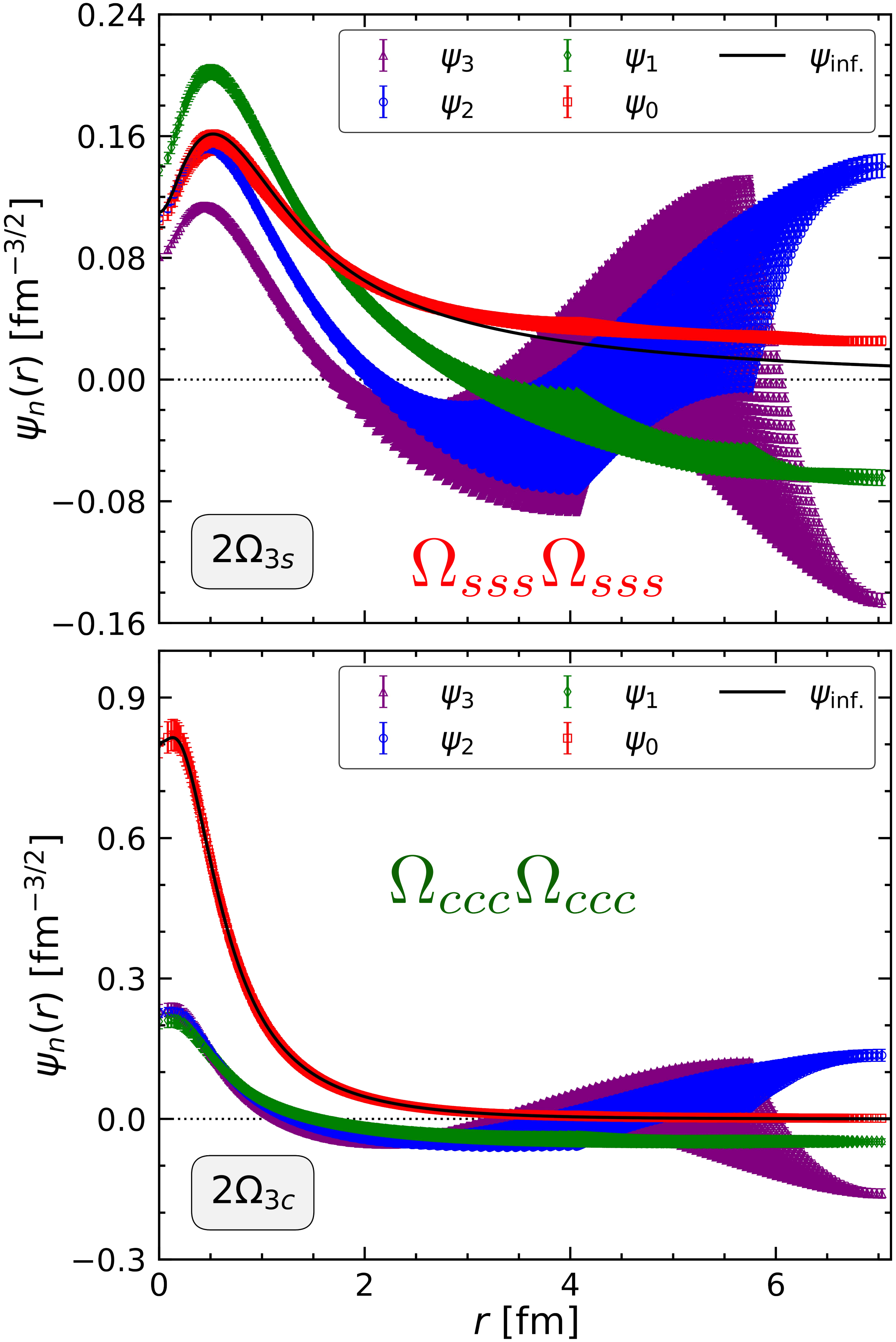

projected wave function $\psi_n(r) := \psi_n(\mathbf{r})|_{r=|\mathbf{r}|}$

a number of nodes $= n$, as expected.

$\ell \geq 4$ components are seen,
in particular for excited states.

A size of the $\Omega_{ccc}\Omega_{ccc}$ ground state is
smaller than that of the $\Omega_{sss}\Omega_{sss}$ ground state.

R-correlator $R(\mathbf{r},t) = \sum_{\mathbf{x}} \langle 0|\Omega(\mathbf{x}+\mathbf{r},t)\Omega(\mathbf{x},t)\mathcal{J}^{\dagger}_{\Omega\Omega}(0)|0\rangle/(Z_{\Omega}e^{-2m_{\Omega}t})$ $\longrightarrow$ potential

sink wall-source

Projected sink operator to n-th eigenfunction

$$S_n(t) := \sum_{\mathbf{r}} \psi_n^{\dagger}(\mathbf{r}) \left[\sum_{\mathbf{x}} \Omega(\mathbf{x}+\mathbf{r},t)\Omega(\mathbf{x},t)\right]$$

Projected R-correlator to n-th eigenfunction

$$R_n(t) := \sum_{\mathbf{r}} \psi_n^{\dagger}(\mathbf{r}) R(\mathbf{r},t) = \langle 0|S_n(t)\mathcal{J}^{\dagger}_{\Omega\Omega}(0)|0\rangle/(Z_{\Omega}e^{-2m_{\Omega}t})$$

n-th Effective energy $\Delta E_n^{\mathrm{eff}}(t) = \frac{1}{a}\ln\left[\frac{R_n(t)}{R_n(t+1)}\right]$

cf. effective energy of R-correlator w/o projection

$$\Delta E^{\mathrm{eff}}(t) = \frac{1}{a}\ln\left[\frac{R(t)}{R(t+1)}\right]$$

$R(t) := \sum_{\mathbf{r}} R(\mathbf{r},t)$ zero momentum projection

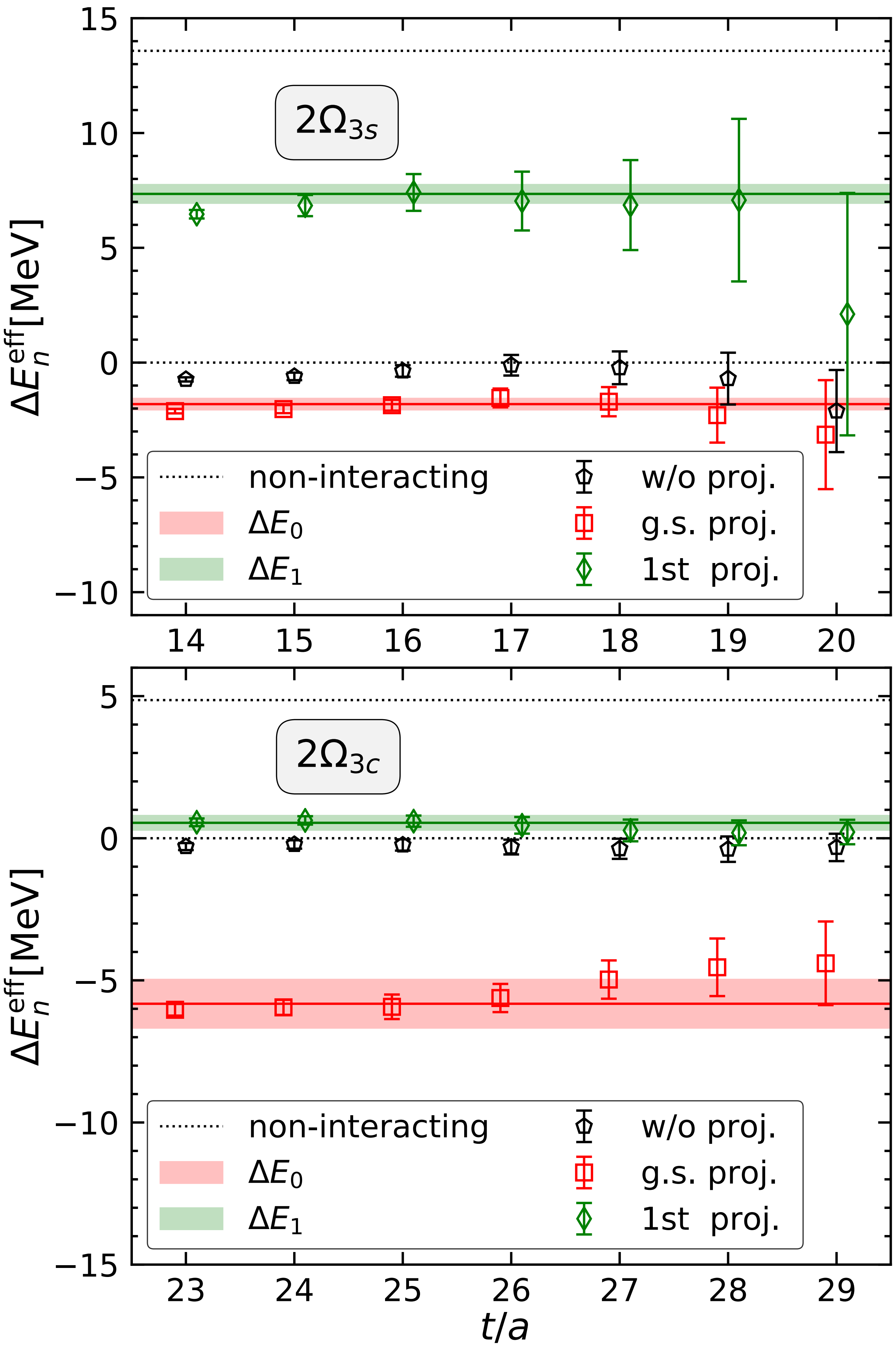

$\Omega_{sss}\Omega_{sss}$

$\Delta E_n^{\rm eff}(t)$ $(n = 0, 1)$ show plateaux behaviors.

$\Delta E_0^{\rm eff}(t)$ agrees with ΔE_0.

FV spectra HAL

$\Delta E_1^{\rm eff}(t)$ is consistent with ΔE_1.

The wall source strongly couples to the ground state.

$\Omega_{ccc}\Omega_{ccc}$

$\Delta E_n^{\rm eff}(t)$ $(n = 0, 1)$ show plateaux behaviors.

$\Delta E_1^{\rm eff}(t)$ agrees with ΔE_1.

FV spectra HAL

$\Delta E_0^{\rm eff}(t)$ is consistent with ΔE_0.

The wall source strongly couples to the 1st excited state.

FV spectra $\simeq$ FV eigenvalues with the HAL QCD potential

Good crosscheck for both methods.

In particular,

systematics from the derivative expansion and inelastic contributions are well under control for the HAL QCD potential.

The potential for $\Omega_{ccc}\Omega_{ccc}$ correctly reproduces the energy of the ground state, even from a small overlap of R-correlator to the ground state.

Decompositions of R-correlator

$$R(\mathbf{r},t) = \sum_n a_n \psi_n(\mathbf{r}) e^{-\Delta E_n t} + \cdots ,$$

$$a_n := e^{-\Delta E_n t_0} \sum_{\mathbf{r}} \psi_n^\dagger(\mathbf{r}) R(\mathbf{r}, t_0)$$

$$R(t) = \sum_n b_n e^{-\Delta E_n t} + \cdots ,$$

$$b_n = a_n \sum_{\mathbf{r}} \psi_n(\mathbf{r})$$

$b_1/b_0 \simeq 0.1$ for $\Omega_{sss}\Omega_{sss}$

the ground state dominates

$b_1/b_0 \simeq 10$ for $\Omega_{ccc}\Omega_{ccc}$

the 1st excited state dominates

$b_n/b_{0,1} < 0.01$ for $n = 2, 3$

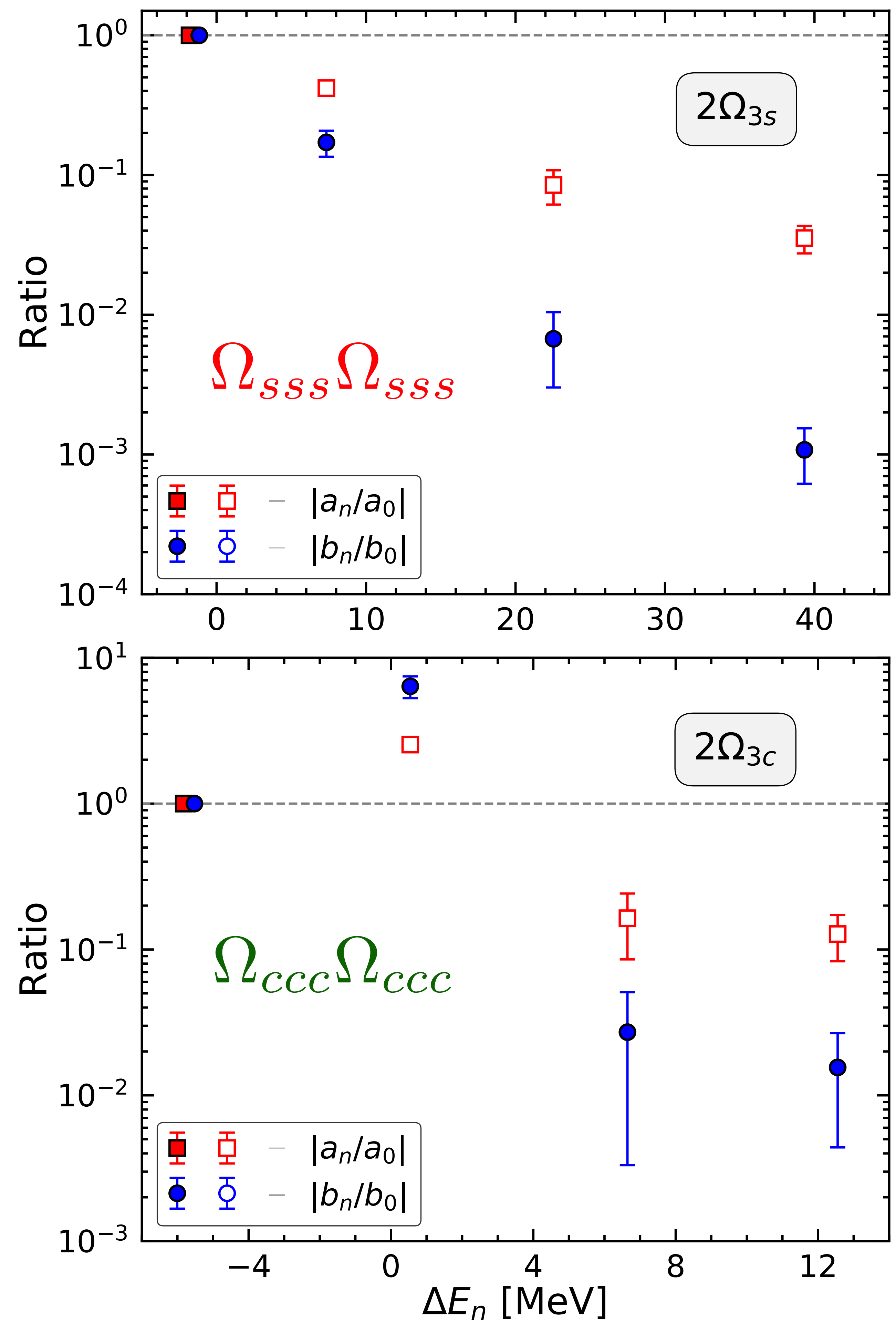

Higher excited states

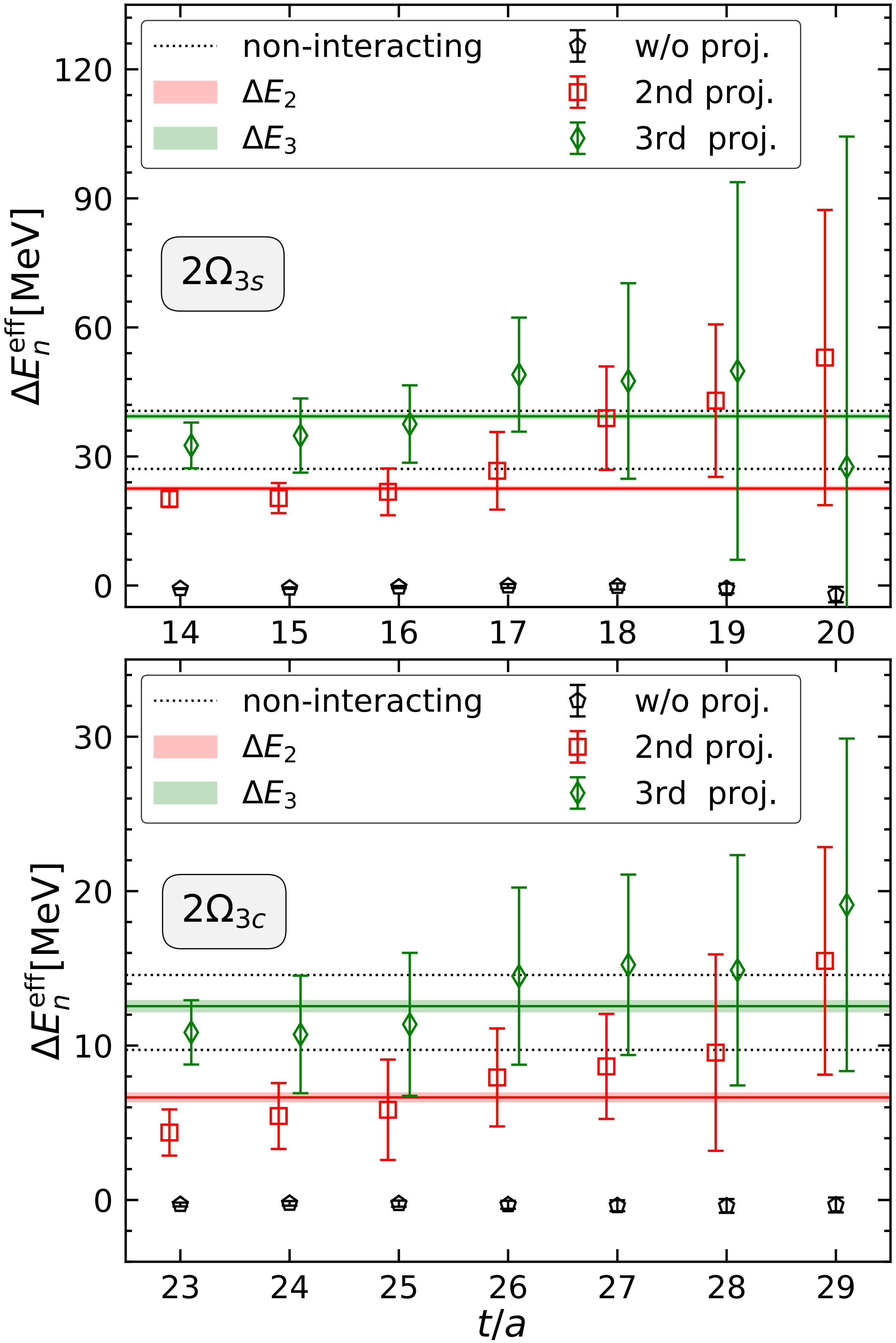

$\Omega_{sss}\Omega_{sss}$

FV spectra are not inconsistent with the HAL QCD spectra for higher excited states, though errors are much larger.

$\Omega_{ccc}\Omega_{ccc}$

V. Conclusions

Conclusions

Since the HAL QCD and the FV methods are complementary, by combining them, we have more confidences on our results of hadron interactions in lattice QCD.

For example, coupled channel (H dibaryon)

(Ambitious) program for improvements

HAL QCD method

Finite volume method

LO potential

projected operators $S_n^{(0)}(t)$

$\Delta E_n^{\mathrm{HAL}_0}$

$\mathrm{GEVP\ for}\ \langle S_n^{(0)}(t) S_m^{(0)}(0)\rangle$

potentials in the derivative expansion

Eigenvalues $\Delta E_n^{\mathrm{FV}_0}$ Eigenoperators $S_n^{(1)}(t)$

using $S_n^{(1)}(0)$ as source operators

If $\Delta E_n^{\mathrm{HAL}_0} \simeq \Delta E_n^{\mathrm{FV}_0}$, stop

new projected operator $S_n^{(2)}(t)$

$\Delta E_n^{\mathrm{HAL}_1}$ If $\Delta E_n^{\mathrm{HAL}_1} \simeq \Delta E_n^{\mathrm{FV}_0}$, stop

$\mathrm{GEVP\ for}\ \langle S_n^{(2)}(t) S_m^{(2)}(0)\rangle$

repeat iterations until it converges

A. Nicolson, Lat2022

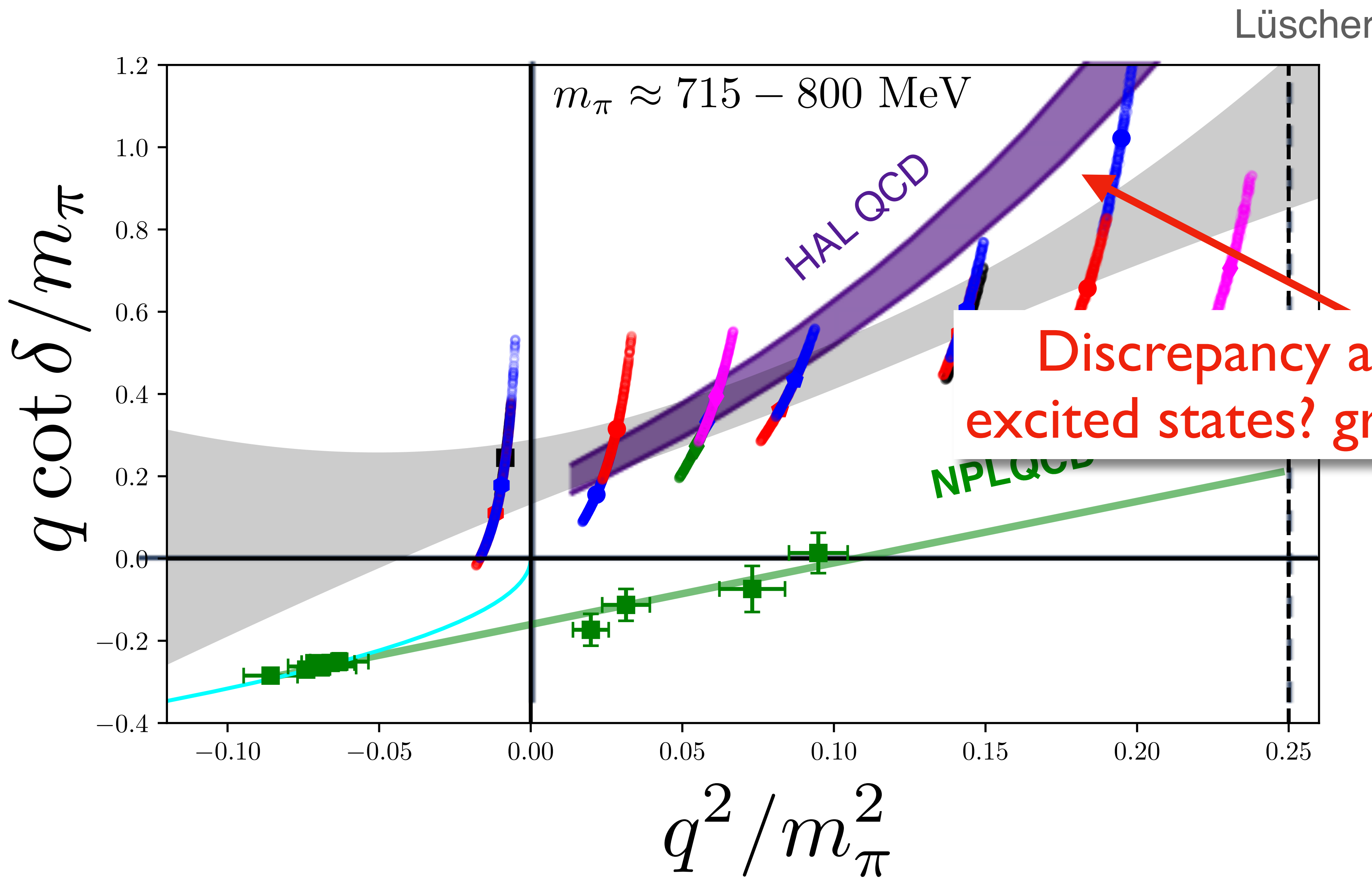

Discrepancy at higher q^2:
excited states? gradient cutoff?

understand this discrepancy by the improved program

Thank you !

Backup

Latest result

Doubly charmed tetraquark T_{cc}^{+} from Lattice QCD near Physical Point

Yan Lyu, *et al.* arXiv:2302.04505

Heavy tetra-quark states T_{cc}

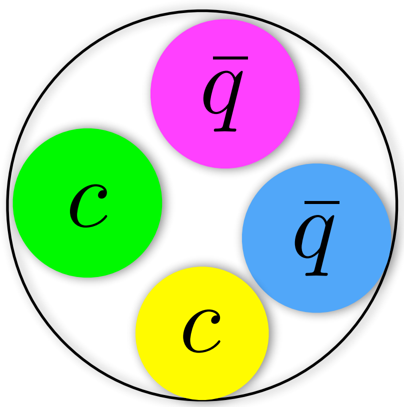

$\bar{q}$: light anti-quark

genuine tetra-quark states

$T_{cc}(cc\bar{u}\bar{d})$ observation by LHCb.

Aaij et al. (LHCb Collaboration) , Nature Phys. (2022)

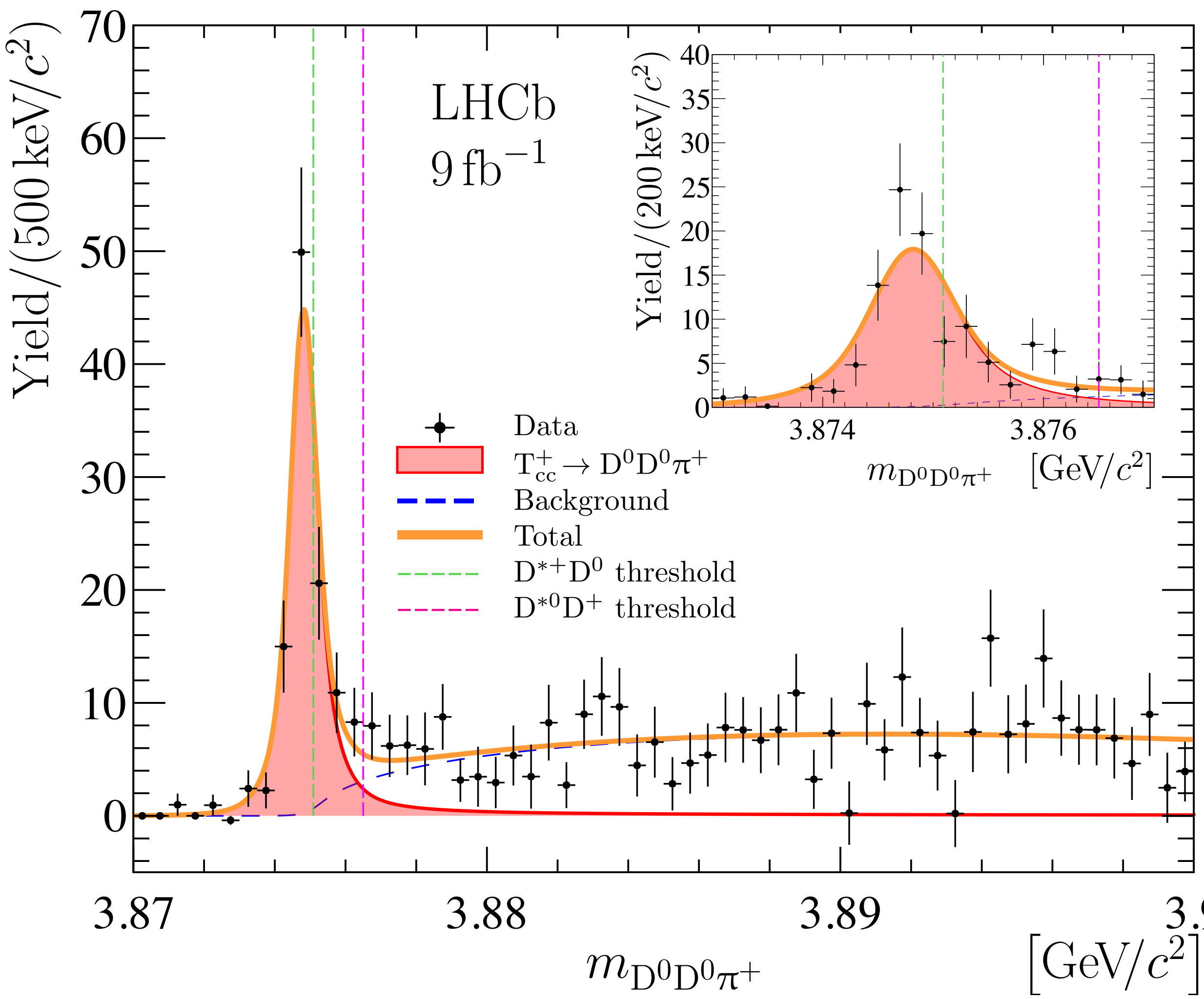

inverse scattering length

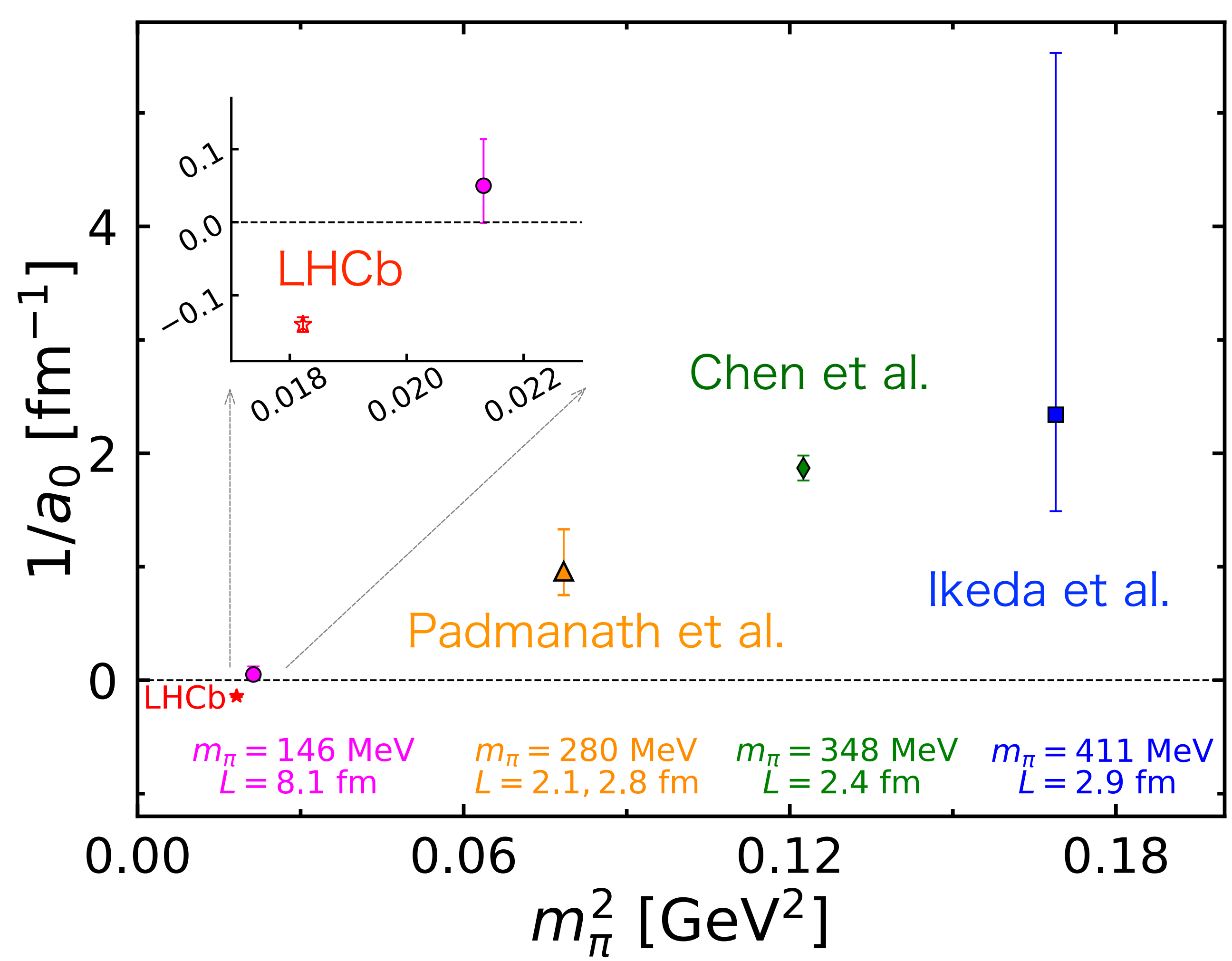

Potentials

$m_\pi \simeq 146$ MeV

D^*D potential

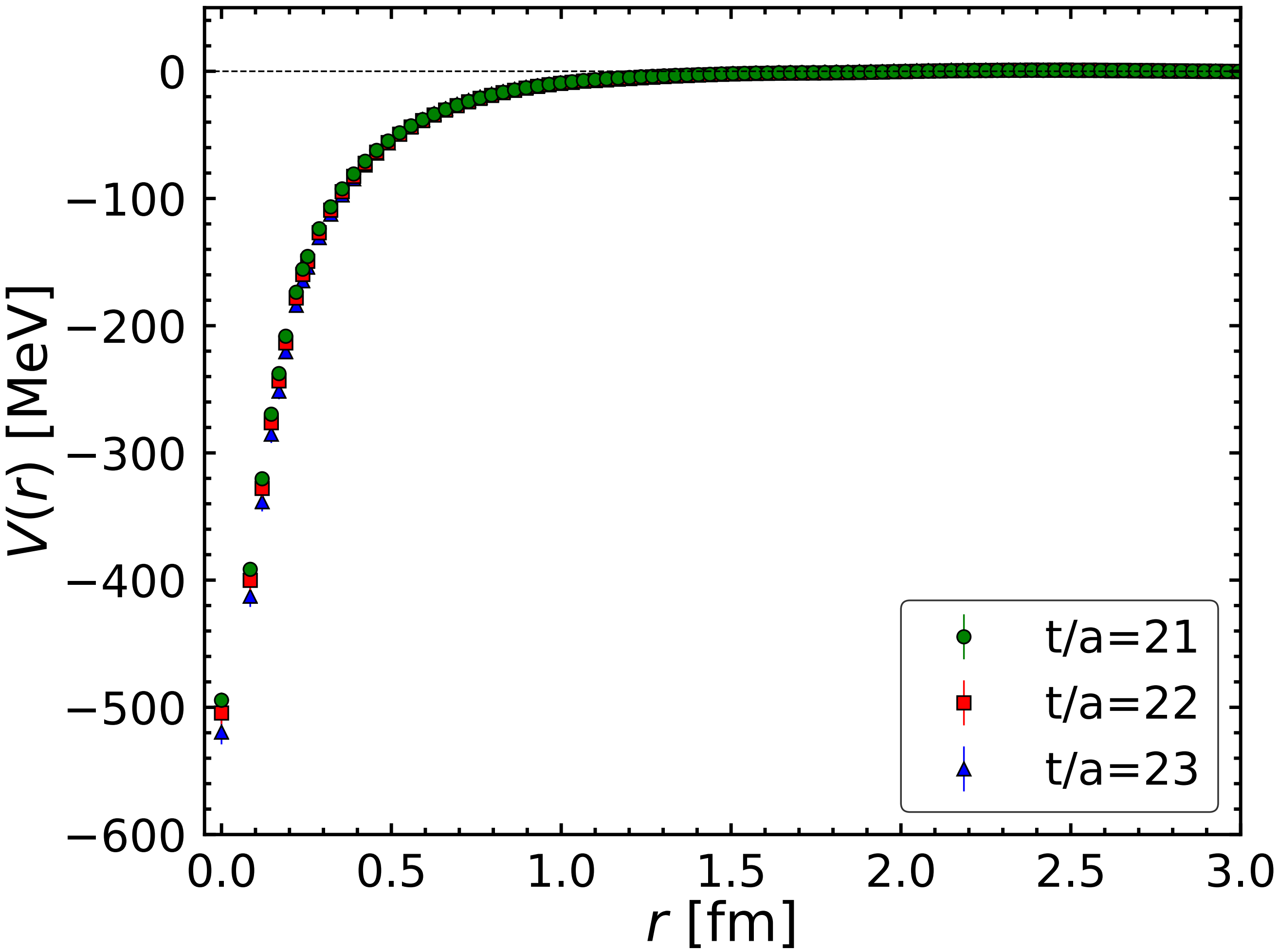

Effective energy in space

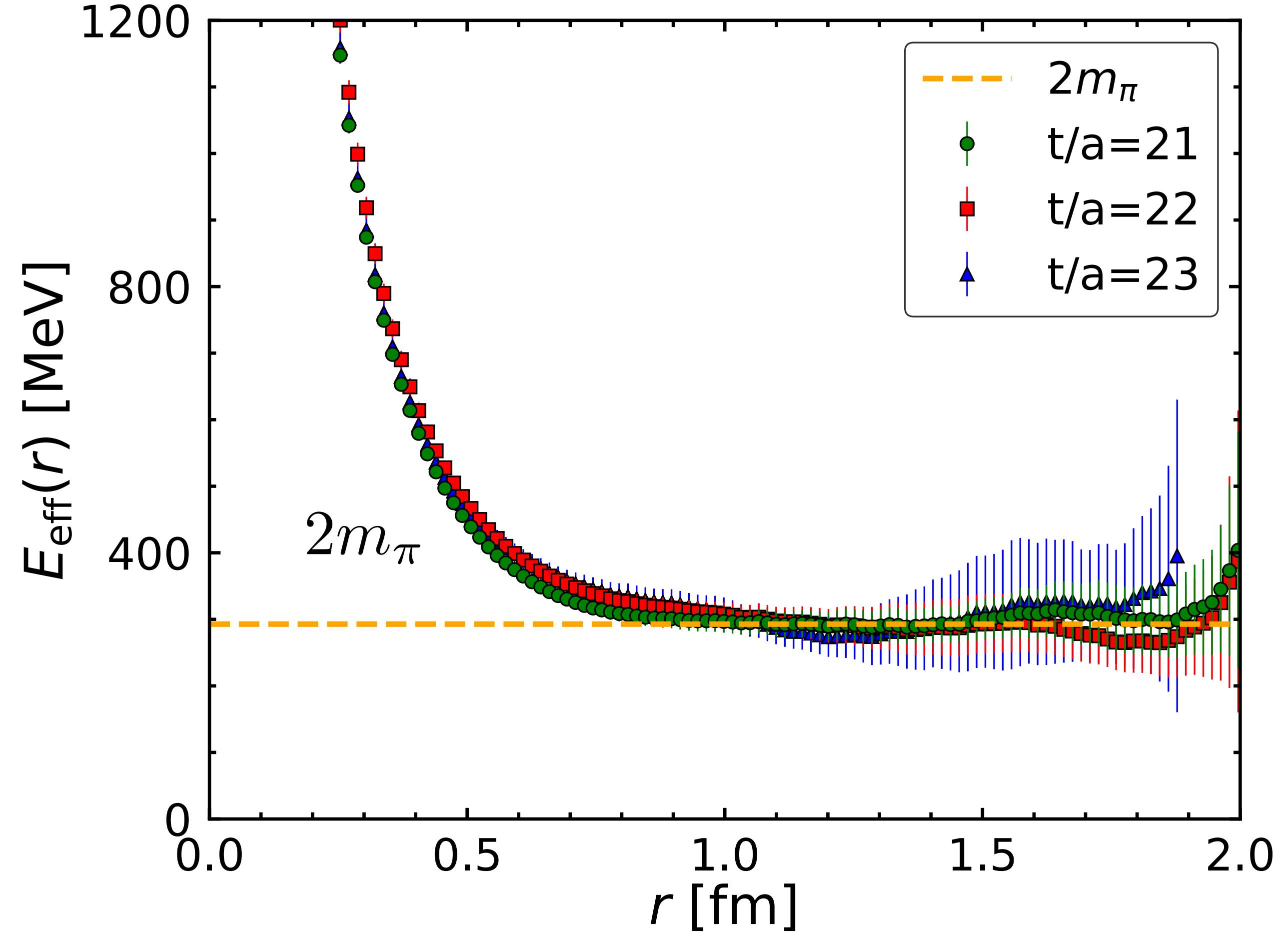

consistent with Yukawa^2 at large r

2-Gauss + Yukawa^2

$$V_{\text{fit}}(r; m_\pi) = \sum_{i=1,2} a_i e^{-(r/b_i)^2} + a_3 (1 - e^{-(r/b_3)^2})^2 \left(\frac{e^{-m_\pi r}}{r} \right)^2$$

Scattering phase shift

$k \cot \delta_0(k)$

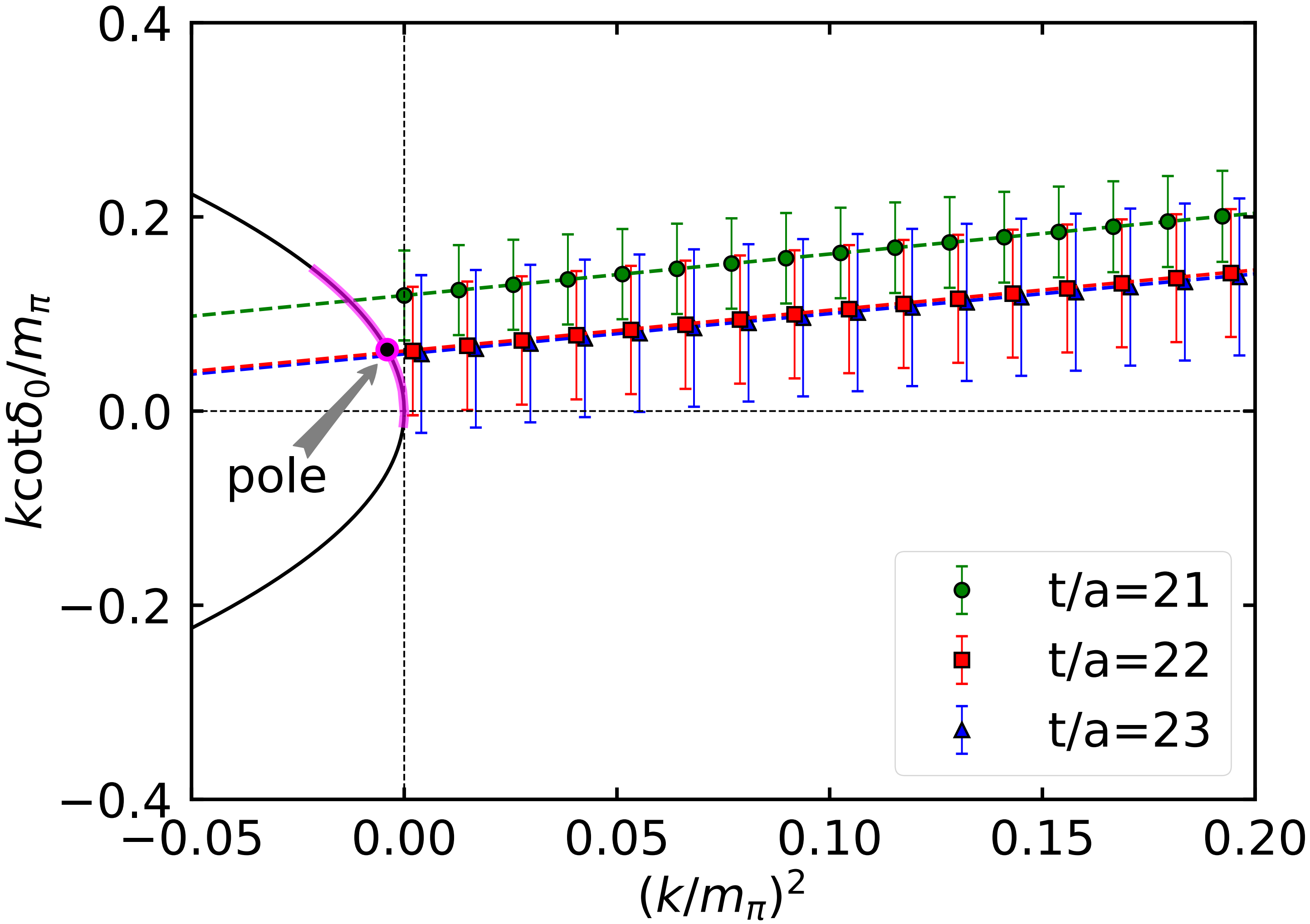

$$k \cot \delta_0(k) = \frac{1}{a_0} + \frac{1}{2} r_{\text{eff}} k^2 + O(k^4)$$

$m_\pi \simeq 146 \text{ MeV}$

one shallow “virtual” state

$$\frac{1}{a_0} \, [\text{fm}^{-1}] = 0.05(5)(^{+4}_{-1})$$

2-Gauss + Yukawa^2

$m_\pi \to 135 \, \text{MeV}$

$$\frac{1}{a_0} \, [\text{fm}^{-1}] = -0.02(4)$$

one shallow bound state

linear chiral extrapolation of $1/a_0$ in m_π^2

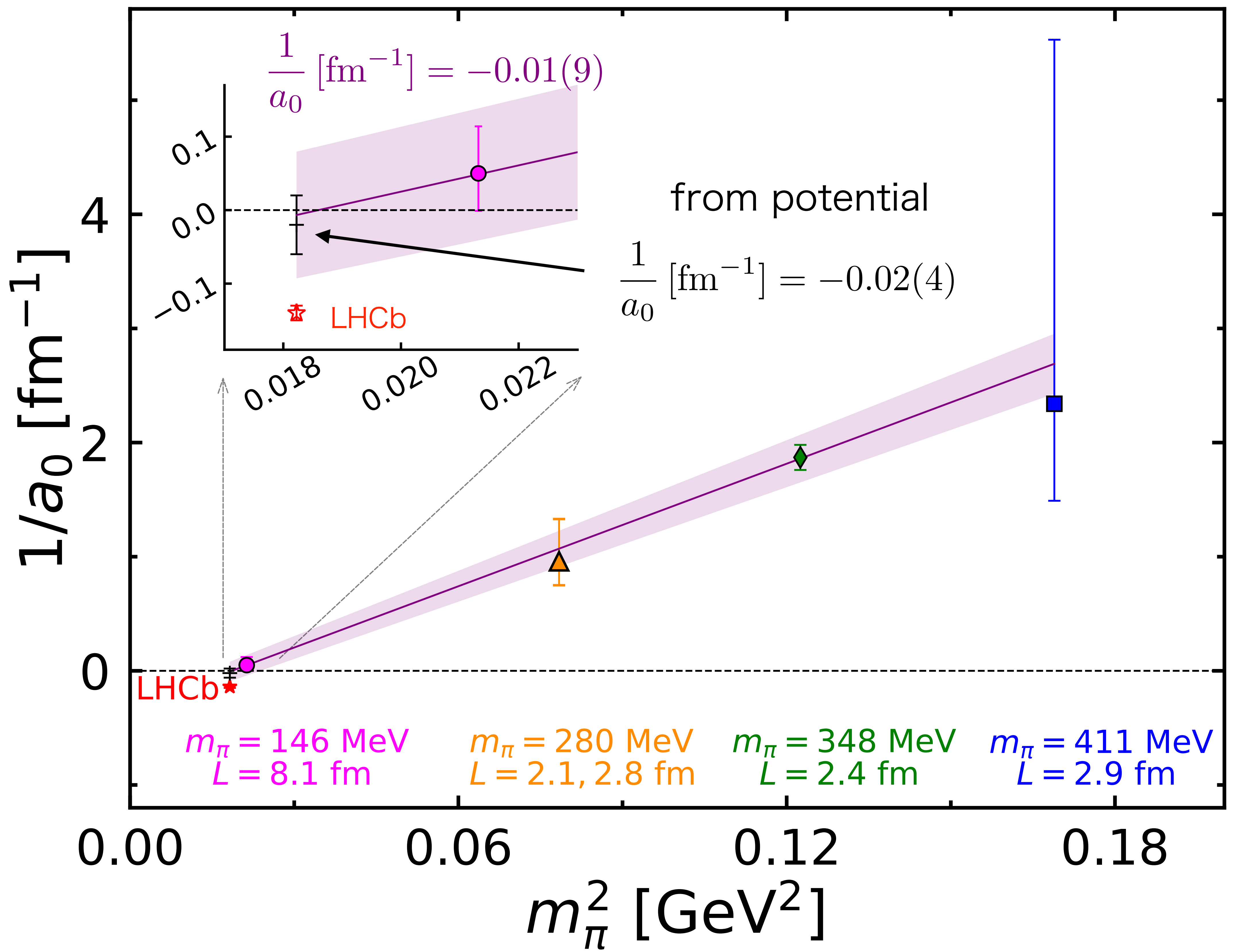

The $D^0D^0\pi^+$ mass spectrum

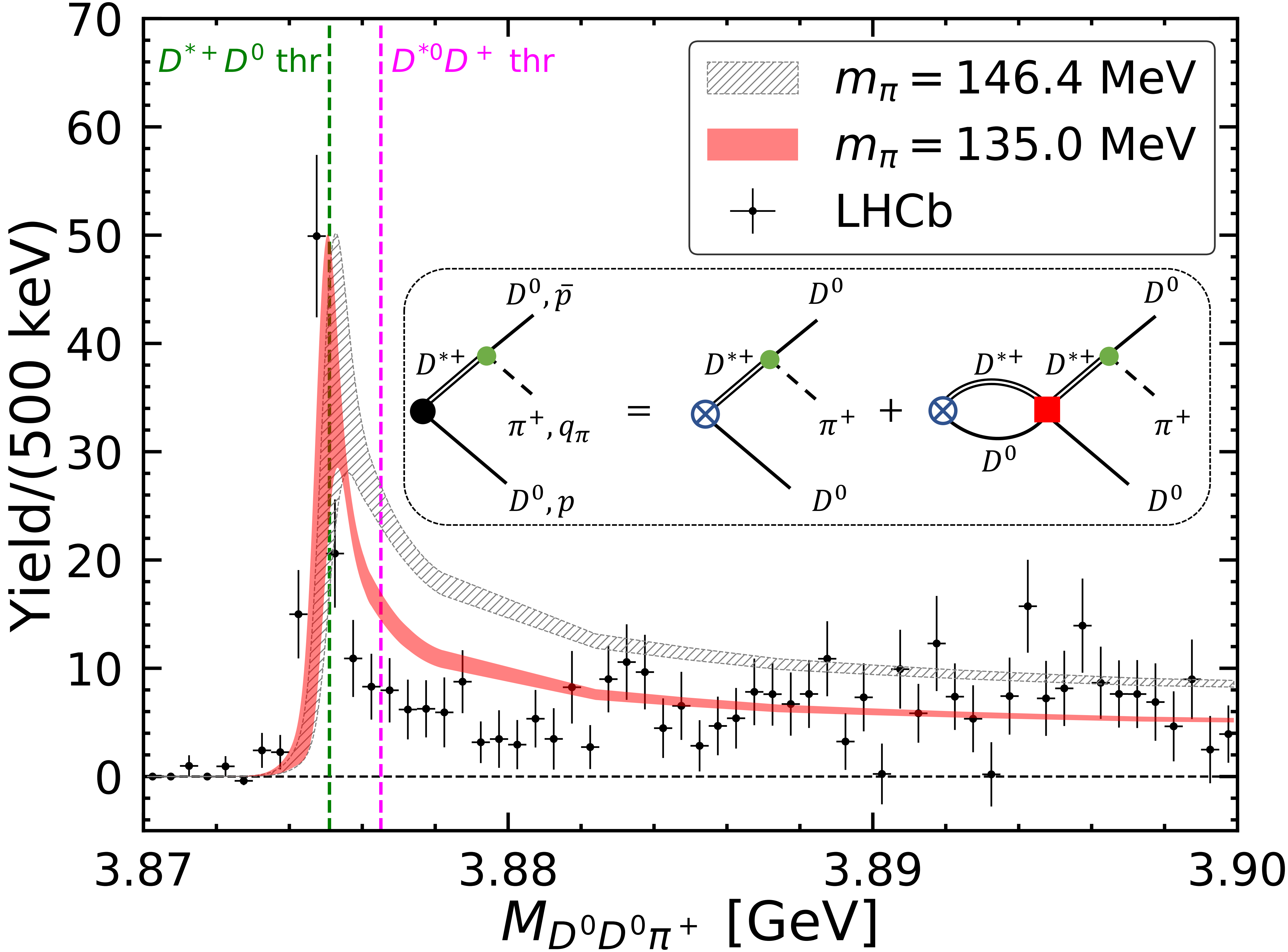

Summary

- A small change in pion mass from 146 MeV to 135 MeV leads to significant changes in physical observables.
  - from a virtual state to a bound state
  - better agreement in the mass spectrum with LHCb
- A more reliable chiral extrapolation is required.
  - configurations at a "physical" pion mass are generated on Fugaku.
  - Stay tuned.